

**FLOW OVER A DELTA WING AND BLUNT BODY COMBINATION  
AT HYPERSONIC SPEEDS**

Amarjit Singh  
College of Aeronautics  
Cranfield University, Cranfield  
Bedford MK43 0AL, U.K.

Abstract

The flow over the lower surface of a wing-body combination with trailing edge flaps was studied using schlieren, and encapsulated liquid crystal techniques along with detailed pressure measurements. The seventy degree swept back delta wing had sharp leading edges and was fitted along the centre line of a blunted cone-cylinder body. The tests were conducted in the College of Aeronautics gun tunnel at  $M_\infty = 8.2$  and  $Re_\infty = 93500 / \text{cm}$ . The model length was 18 cm. The angle of attack of the model was varied from 0 to  $10^\circ$  for flap deflection angles ranging between 0 and  $25^\circ$ . The results indicated large separated regions on the wing. Comparison with other data showed how the body nose bluntness changed the trailing edge flap effectiveness.

Symbols

- $\alpha$  angle of attack
- $\beta$  flap deflection angle
- $\bar{\chi}$  viscous interaction parameter
- M Mach number
- Re. Reynolds number
- S distance along chord
- Y distance along span
- Cr root chord
- b half span
- Subscripts
- $\infty$  free stream conditions
- i incipient separation

Introduction

The body nose is known to effect the entire flow field around an aerospace vehicle. A number of studies have been made regarding the influence of nose bluntness on the flare effectiveness of a cone-cylinder-flare body. Numerical calculations by Ashby and Cary<sup>(1)</sup> using the method of

characteristics showed that blunting the nose of a cone cylinder body creates a region of low constant-dynamic-pressure near the surface of the body. In between this low dynamic pressure region and the bow shock wave the dynamic pressure rises rapidly. The effectiveness of the flare is therefore dependent upon the size of the flare, relative to the size of the low total pressure region around the body, created by the bow shock wave. An experimental study of the flow around a wing-body model is being made to investigate the effect of body nose bluntness on the trailing edge flap effectiveness. This paper reports the flow visualisation using a single pass Schlieren system and the liquid crystal technique and detailed surface pressure measurements on the windward surface of the wing and flap.

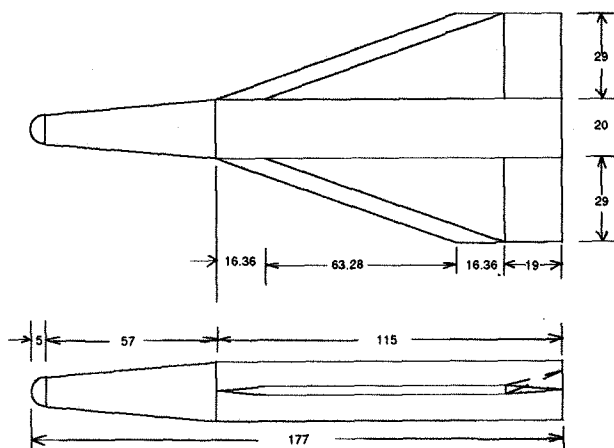


Figure 1. Wing- body model  
All dimensions are in mm.

Experimental facility

The experiments were conducted in the College of Aeronautics gun tunnel. The axisymmetric nozzle provided a useful jet of 15 cm diameter at  $M_\infty$  of 8.2 and  $Re_\infty$  equal to 93500/cm. For surface flow visualisation encapsulated liquid crystals were sprayed on the matt black painted

aluminium model. The model was illuminated by an ordinary camera flash. A single photograph was taken just before the end of each run using a single shot camera. Electrical, strain gauge type, pressure transducers were used for the pressure measurements. The pressure transducers were calibrated against a vacuum gauge before each run.

## Results and discussion

### Flow visualisation

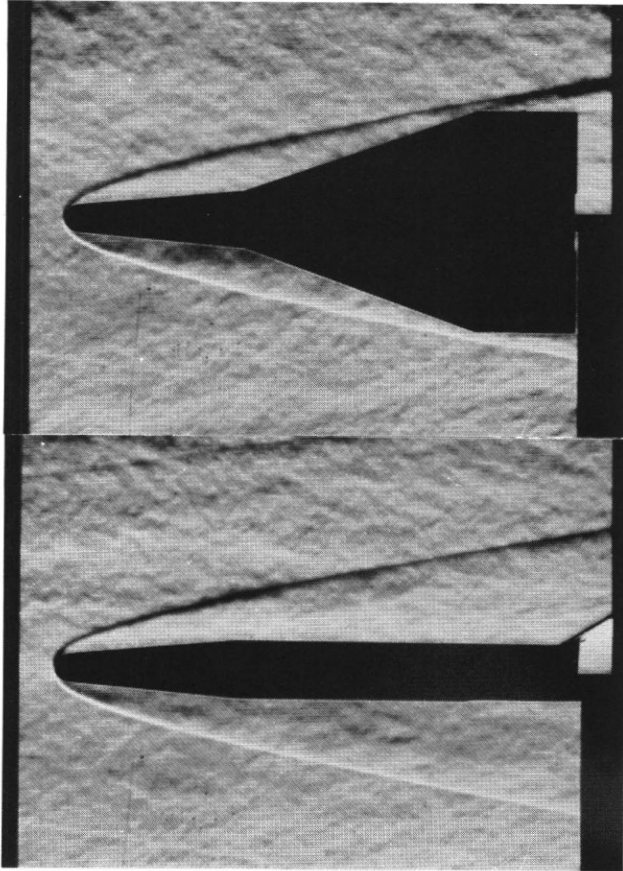


Figure 2. Schlieren pictures showing top and side view for  $\alpha = 0^\circ$  and  $\beta = 25^\circ$ .

The Schlieren pictures in figures 2 and 3 show the top and side view of the wing-body model for a flap deflection angle,  $\beta=25^\circ$  and angles of attack,  $\alpha = 0$  and  $10^\circ$  respectively. The body shock at  $\alpha = 0^\circ$  was estimated using blast wave theory. The theory was found to slightly underestimate the position of the bow shock wave. The wing leading edge shock is attached at  $\alpha = 0$  and  $5^\circ$  but gets detached at  $\alpha = 10^\circ$ .

This compared well with the prediction based upon the method given by Stetson and Scaggs.<sup>(2)</sup> The liquid crystal technique was used to get qualitative information about the heat transfer rates on the wing-body model. The technique was first tried on a rectangular planform plate with a sharp leading edge and a trailing edge flap. The location of colour change on the model was determined visually from the still camera photographs. A comparison of heat transfer measurements on the flat plate using thin film

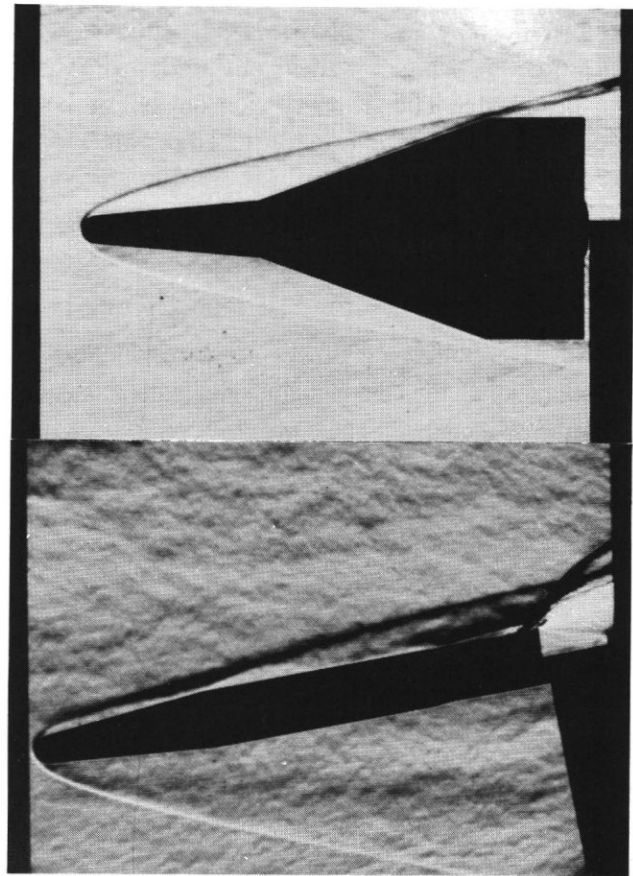


Figure 3. Schlieren pictures showing top and side view for  $\alpha = 10^\circ$  and  $\beta = 25^\circ$ .

gauges and liquid crystal colour change positions was very encouraging and the technique was then used for qualitative flow visualisation on the wing-body model.

### Unseparated flow

The two-dimensional laminar flow correlation<sup>(3)</sup> given below was used to estimate the incipient separation angle for the wing-body model.

$$M_\infty \beta_i = 80 \lambda^{0.5}$$

This correlation predicted  $\beta_1 = 7.5, 6.2,$  and  $5.5^\circ$  for  $\alpha = 0, 5,$  and  $10^\circ$  respectively. To calculate  $\bar{\chi}$  at  $\alpha \neq 0$  the local values behind an oblique shock were used for  $M, Re,$  etc. The pressure measurements and the liquid crystal photographs confirmed the flow to be attached for  $\beta = 5^\circ$  at  $\alpha$  equal to  $0, 5,$  and  $10^\circ$ . The pressure distributions

pressure is attained near the most outward location which should be least effected by the entropy layer.

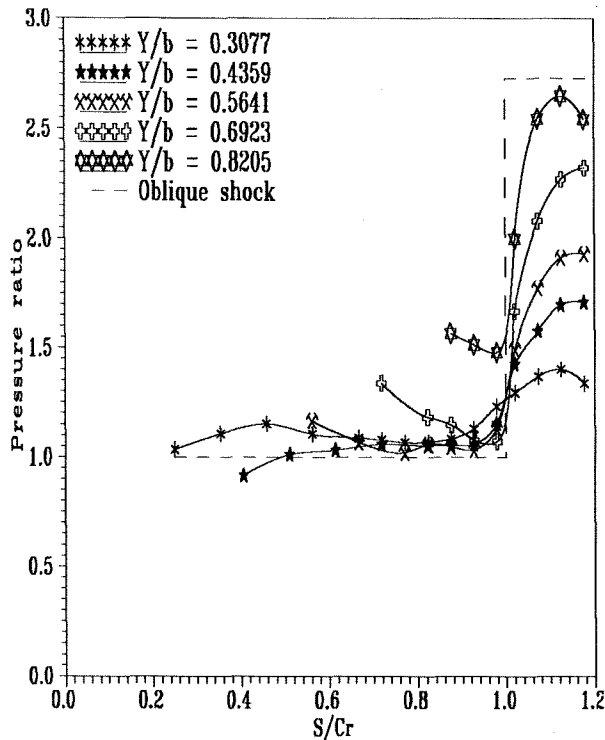


Figure 4. Chord wise pressure distribution at various span wise locations,  $\alpha=0$  and  $\beta=5^\circ$ .

over the wing for  $\beta = 5^\circ$  and  $\alpha = 0$  and  $10^\circ$  are shown in figures 4 and 5 respectively. For  $\alpha = 0$  the pressure on the wing is nearly equal to the free stream pressure except at the spanwise location near the tip. There is an appreciable increase in pressure near the wing leading edge mainly due to wing cross sectional shape. Tangent cone theory is generally found to give a better estimate of the wing pressure for  $\alpha \neq 0$  (6). However, figure 5 indicates that the oblique shock estimation is better than that of the tangent cone over most of the spanwise locations on the wing. Figures 4 and 5 show that the pressure starts increasing just ahead of the hinge line but the maximum pressure attained on the flap is well below the oblique shock value. The highest

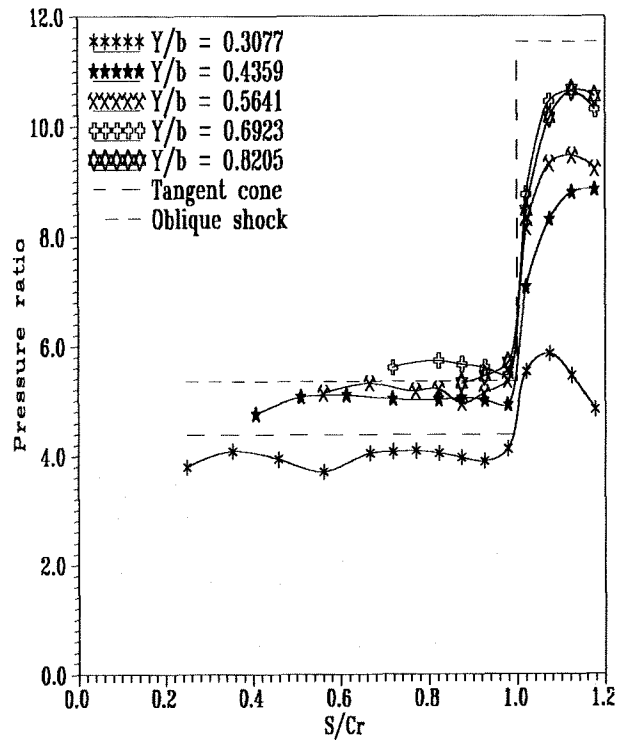


Figure 5. Chord wise pressure distribution at various span wise locations,  $\alpha=10$  and  $\beta=5^\circ$

#### Separated flow

The equation given below has been found to give a good fit of the correlated plateau pressure data at Mach numbers up to 15. (6)

$$C_p \text{ plateau } (M^2 - 1)^{.25} = 1.74 Re^{-.25}$$

This equation was used to estimate plateau pressure based upon local Reynolds number,  $Re,$  at the hinge line. Figures 6 and 7 show the chord wise pressure distribution at the span wise location  $Y/b = 0.5641$  for  $\beta = 0, 5, 15,$  and  $25^\circ$  at  $\alpha = 0$  and  $10^\circ$ . The correlation seems to give a good estimate of the plateau pressure for the complex three dimensional flow conditions over the wing-body model. The experimental plateau pressure values for inward stations, highly effected by the entropy layer effects, were found to be below the values predicted by the above

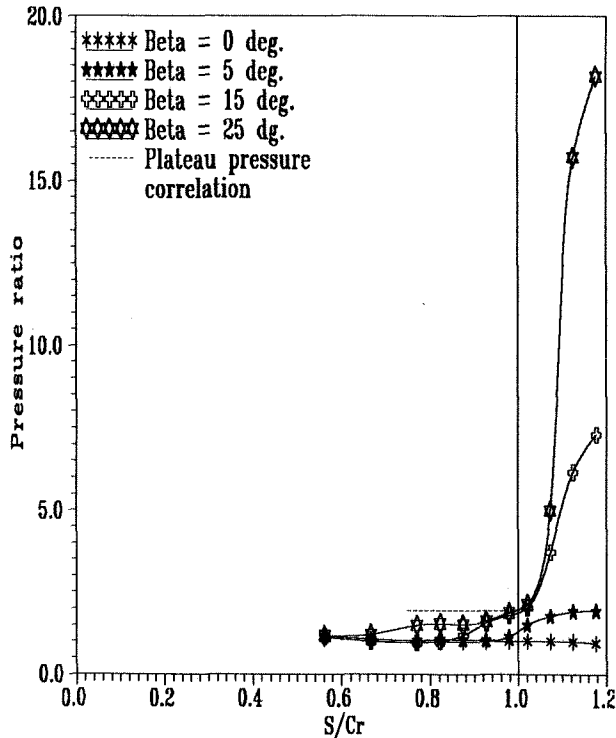


Figure 6. Chord wise pressure distribution at span wise location  $Y/b = 0.5641$ ,  $\alpha=0$  and  $\beta=0, 5, 15$  and  $25^\circ$ .

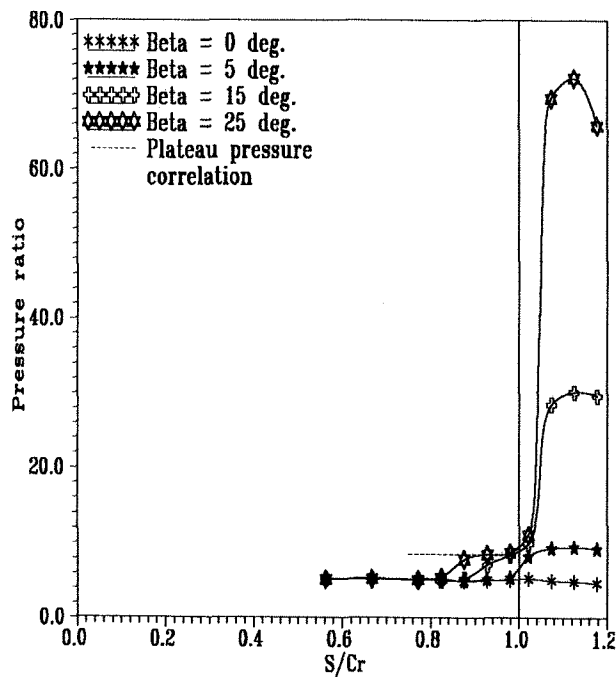


Figure 7. Chord wise pressure distribution at span wise location  $Y/b = 0.5641$ ,  $\alpha=10$  and  $\beta=0, 5, 15$  and  $25^\circ$ .

correlation. An increase in flap angle from 0 to  $25^\circ$  increases the length of the plateau pressure region. Together with the liquid crystal photographs, it can be concluded that the increase in flap angle shifts the separation point forward on the wing. The trend was similar for the other incidences and spanwise locations. Figures 8, and 9 show the pressure distribution on the wing for  $\beta = 25^\circ$  at  $\alpha = 0$  and  $10^\circ$ . The

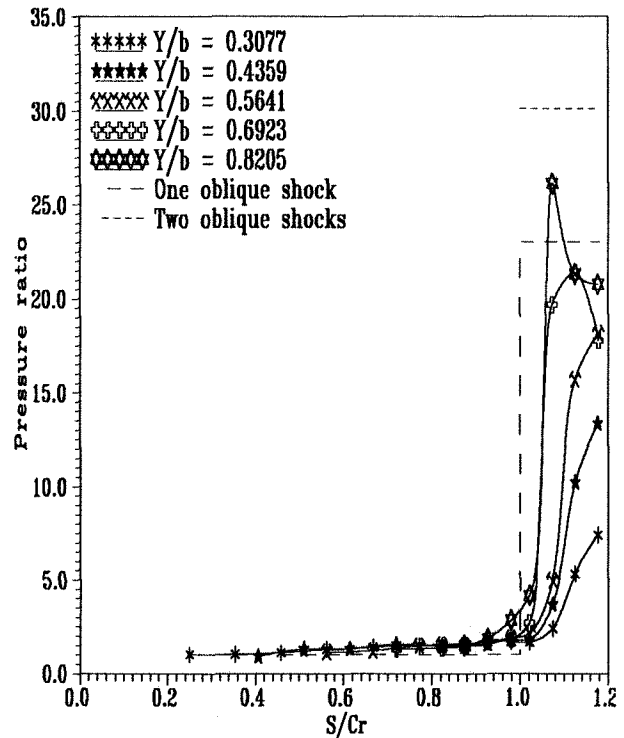


Figure 8. Chord wise pressure distribution at various span wise locations,  $\alpha=0$  and  $\beta=25^\circ$ .

pressure distribution and the liquid crystal pictures indicate the flow to be separated well ahead of the hinge line at  $\alpha = 0^\circ$ . An increase in  $\alpha$  to  $10^\circ$  moves the separation line towards the hinge line. The liquid crystal pictures and pressure distributions also suggest that reattachment occurs on the flap nearer to the hinge line for  $\alpha = 10^\circ$  than for the  $\alpha = 0^\circ$  case. Thus the separation length is decreasing with an increase in  $\alpha$  and hence with an increase in local Reynolds number over the wing. This suggests

that the flow may be transitional at  $\alpha = 10^\circ$ .

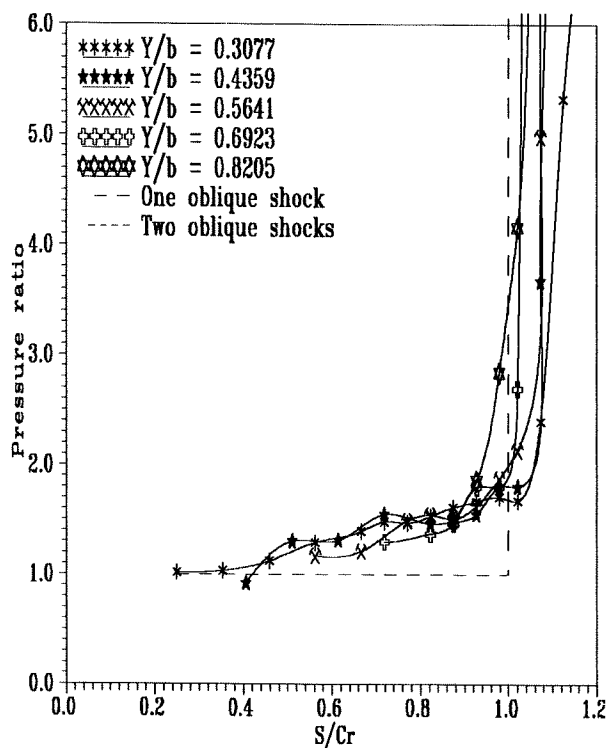


Figure 8. Chord wise pressure distribution at various span wise locations,  $\alpha=0$  and  $\beta=25^\circ$ .

Only for the spanwise stations near the tip ( $\alpha=0^\circ$ , and  $\beta=25^\circ$ ) do the pressure levels reach the oblique shock values. However, for  $\alpha = 10$ , and  $\beta=25^\circ$  the oblique shock values are reached over most of the flap span. The decrease in pressure beyond the peak is probably due to the shock interactions. The reflected expansion waves from the interaction between the separation and reattachment shocks is likely to be hitting the flap surface, resulting in a sudden fall in pressure. An increase in  $\alpha$  moves the bow shock nearer to the windward surface of the wing and most of the 25 degree flap is then unaffected by the entropy layer caused by the body nose bluntness, as could be seen in figures 8 and 9.

### Conclusions

The entropy layer created by the body nose bluntness reduces the peak pressures obtainable on the flap. This will adversely effect the trailing edge flap effectiveness. The flap effectiveness will vary with the flap angle as well as the body angle of attack.

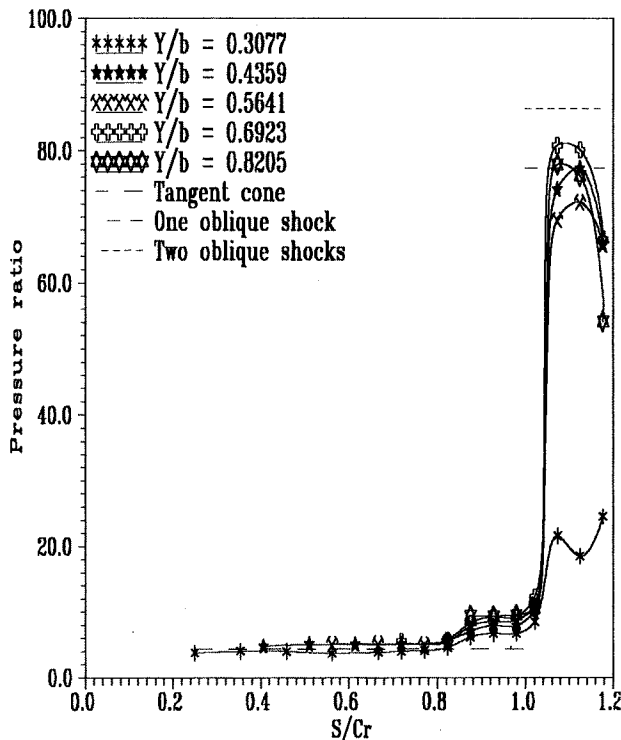


Figure 9. Chord wise pressure distribution at various span wise locations,  $\alpha=10$  and  $\beta=25^\circ$ .

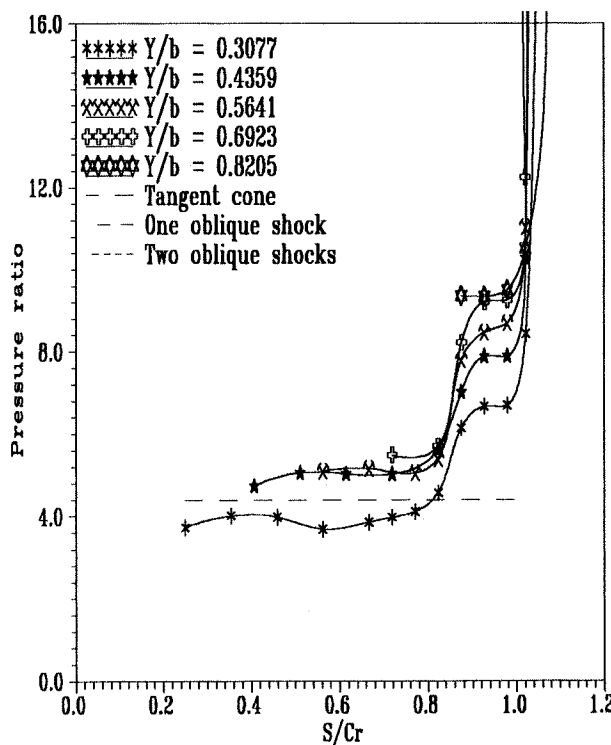


Figure 9. Chord wise pressure distribution at various span wise locations,  $\alpha=10$  and  $\beta=25^\circ$ .

### References

1. Ashby, G. C. and Cary, A. M. A parametric study of the aerodynamic characteristics of nose-cylinder-flare bodies at Mach number of 6.0. NASA TN D-2854, June, 1965.
2. Stetson, K. F. and Scaggs, N. E. Shock detachment from the leading edge of delta wings. ARL 72-0079, 1972.
3. Needham, D. A. and Stollery, J. L. Boundary layer separation in hypersonic flow. AIAA paper 66-455, 1966.
4. Needham, D. A. and Stollery, J. L. Hypersonic studies of incipient separation and separated flows. ARC 27 752, 1966.
5. Whitehead, A. H. and Keyes, J. W. Flow phenomena and separation over delta wings with trailing edge flaps at Mach 6. AIAA Journal Vol. 6, No. 12, Dec., 1968, pp 2380-2387.
6. Rao, D. M. Hypersonic control effectiveness studies on delta wings with trailing edge flaps. Ph.D. thesis, University of London, 1970.